New Optical Sensor Suite for Ultrahigh Temperature Fossil Fuel Applications

Semiannual Technical Progress Report

DOE Award Number: DE-FC26-03NT41922

Reporting Start Date: 1 May 2006

Reporting Period End Date: 30 September 2006

Principal Authors: John Coggin
Jonas Ivasauskas
Russell G. May
Michael B. Miller
Rena Wilson

Date Report Issued: 31 October 2006

Submitting Organization: Prime Research, LC
1750 Kraft Dr Ste 1000
Blacksburg, VA 24060

DISCLAIMER

This report was prepared as an account of work sponsored by an agency of the United States Government. Neither the United States Government nor in the agency thereof, nor any of their employees, makes any warranty, express or implied, or assumes any legal liability or responsibility for the accuracy, completeness, or usefulness of the information, apparatus, product, or process disclosed, or represents that its use would not infringe privately owned rights. Reference herein to any specific commercial product, process, or service by trade name, trademark, manufacturer, or otherwise does not necessarily constitute or imply its endorsement, recommendation, or favoring by the United States Government were in the agency thereof. The views lists opinions of authors expressed herein do not necessarily state or reflect those of United States Government or any agency thereof.

ABSTRACT

Accomplishments during Phase II of a program to develop and demonstrate photonic sensor technology for the instrumentation of advanced powerplants are described. The goal of this project is the research and development of advanced, robust photonic sensors based on improved sapphire optical waveguides, and the identification and demonstration of applications of the new sensors in advanced fossil fuel power plants, where the new technology will contribute to improvements in process control and monitoring. During this program work period, major progress has been experienced in the development of the sensor hardware, and the planning of the system installation and operation. The major focus of the next work period will be the installation of sensors in the Hamilton, Ohio power plant, and demonstration of high-temperature strain gages during mechanical testing of SOFC components.

TABLE OF CONTENTS

1 INTRODUCTION

The goal of this project is the research and development of advanced, robust photonic sensors based on improved sapphire optical waveguides, and the identification and demonstration of applications of the new sensors in advanced fossil fuel power plants, where the new technology will contribute to improvements in process control and monitoring.

The advantages of fiber optic sensors over electronic sensors, particularly in environments where the electronic sensing materials can not withstand the rigors of the harsh conditions, are well known. Typically, advanced power generation systems operate at higher temperatures and pressures than traditional power plants. Traditional sensor technology for measuring temperature, pressure, flow and strain will not survive the harsh conditions anticipated in these plants. Furthermore, these plants will require more extensive process monitoring and condition assessment to maintain optimum performance and minimize maintenance costs. An effective means is required to reduce the complexity and cost of connecting the larger number of sensors to a central data acquisition platform. Therefore, one of the goals of the program is the identification of all potential applications in supercritical boiler plans where photonic sensors can be used for process control and monitoring.

For the ultrahigh-temperature environment found in current and future power generation facilities, new materials for the optical sensors will be required. Previous efforts to utilize sapphire fiber sensors that can theoretically operate above 1650° C (3000° F) have been limited because the fiber itself does not lend itself to incorporation in the known sensor techniques, due to its unclad and multimode construction. Another goal of this program is the development of high-temperature, ceramic claddings for sapphire fibers to improve the waveguiding properties of sapphire fibers and facilitate their use in photonic sensor systems.

Current efforts towards improvement of sapphire fibers focus on creating claddings on sapphire (aluminum oxide single crystal, Al_2O_3) fibers by dip-coating the fibers in a mixture of magnesium oxide (MgO) powders and magnesium aluminate spinel ($MgAl_2O_4$) powders to form a coating on the sapphire fibers. The technique involves dip coating a sapphire fiber in a suspension of MgO and spinel powders, drying the coating, then firing at elevated temperatures to react the MgO powder with the sapphire fiber, and to densify the coating. The overall reaction for the process is given by the chemical equation:

$$MgO + Al_2O_3 = MgAl_2O_4$$

which proceeds rapidly at 1750°C (3182° F).

The coated fibers are then fired at high temperatures to facilitate the reaction between the MgO in the coating and the Al_2O_3 in the fibers by ion diffusion, and create a cladding consisting of $MgAl_2O_4$ surrounding the sapphire core. As a result, the diameters of the sapphire fibers are reduced and the number of modes propagating in the sapphire fibers is also reduced.

2 EXECUTIVE SUMMARY

During this program work period, progress was made in the design, development, and testing of high-temperature photonic sensors for instrumentation of advanced fossil fuel power plants and solid oxide fuel cells.

High-temperature packaging was designed to protect sapphire temperature and strain sensors during installation of the sensors in the Hamilton, OH coal-fired boiler plant. The sensor housings will be based on inconel, an oxidation-resistant and corrosion-resistant high-nickel alloy, and alumina, a refractory ceramic. The packages were designed to reinforce critical joints in the optical assembly and maintain optical alignment in operation. In addition, techniques for installing the sensors were developed, and mounting adapters to attach the sensors to desired locations in the plant were designed. Three locations will be instrumented with one temperature sensor and one strain gage in each location: on a bracket supporting the secondary superheater tube bank, in the membrane wall adjacent to the secondary superheater tube bank, and then on a crossover pipe above the boiler penthouse.

Algorithms were investigated for processing the spectral responses of Fabry-Perot sensors to yield absolute measurements (in which no data regarding the sensor history is required to obtain an accurate measurement of the environment), as opposed to relative measurements (which give only the change from a previous measurement). One method investigated was shown to achieve absolute measurements for spectra obtained from Fabry-Perot sensors made from silica fibers. Tests with Fabry-Perot sensors made from sapphire fibers, however, indicated that the complex spectra exhibited by sapphire Fabry-Perot sensors confounded the algorithm. Work is continuing in order to develop digital filters optimized for processing spectra from sapphire Fabry-Perot cavities.

Tests were performed to assess the maximum operating temperature for splices made between silica fibers and sapphire fibers that were developed in the last reporting period. The splice was found to operate successfully to 842° F (450° C). Further tests were performed to determine the maximum temperature that the splice will experience after installation and during operation of the sapphire sensors in the Hamilton, Ohio power plant. By measuring the temperature profile of the sensor housing that protrudes out of the boiler wall, it was determined that the splice should be located no closer than 1.5 inches (38 mm) from the membrane wall of the boiler plant.

Development of strain sensors for the instrumentation of solid oxide fuel cells for mechanical testing of fuel cell components continued during the reporting period. Fabry-Perot strain gages based on micromachined fused silica optical fibers were evaluated. Several adhesives for bonding the optical strain gauge to the solid oxide fuel cell substrate were investigated, and a ceramic adhesive with a silica filler was found to provide the best strain transfer fidelity, and to give the most stable measurements at temperatures up to 1,472° F (800° C).

During the reporting period, work was initiated in the development of technologies to measure the distribution of temperature and strain across the surface of solid oxide fuel cell components. By concatenating multiple sensor elements along a single optical fiber, and applying optical signal processing methods to deconvolve and separate the responses of the individual sensors, the temperature and/or strain distribution across the fuel cell component may be mapped. Instrumentation of a bipolar plate for mapping temperature distribution has been adopted as the goal for first demonstration. After considering various candidate methods for sensor designs, a weakly-reflecting intrinsic Fabry-Perot interferometer (IFPI) was chosen as the most promising sensor type for the proposed application. In the next reporting period, the use of a high-powered excimer laser to write persistent, high-temperature IFPI cavities in photosensitive fibers will be explored. In addition, signal processing algorithms based on optical time domain reflectometry and optical frequency domain reflectometry will be investigated, to determine the optimal method for deconvolving the responses of serial Fabry-Perot cavities.

3 EXPERIMENTAL PROGRESS

3.1 Development of Sensors for Power Plant Instrumentation

During this reporting period, progress was made in the development of protective packaging for the sapphire strain gage and temperature sensor, and procedures were developed for the installation of the sensors in the Hamilton, Ohio power plant.

3.1.1 Sapphire Temperature Sensor Development

Extending upon the optical design for the sapphire temperature sensor described in the last semiannual report, a package was designed to facilitate sensor installation and protect the sensor in use. The package for the temperature sensor was designed to withstand the high temperatures and corrosive atmosphere of the furnace, conduct heat efficiently, and protect the sapphire sensing element from dust, shock, and vibration.

The housing and tip illustrated in Figure 1 are to be fabricated of inconel, a high nickel alloy with properties making it well suited for service in this extreme environment. Inconel is very resistant to oxidation and corrosion. When heated, inconel forms a stable passivating oxide layer protecting it from further attack. Inconel retains its strength at the high temperatures experienced in this environment.

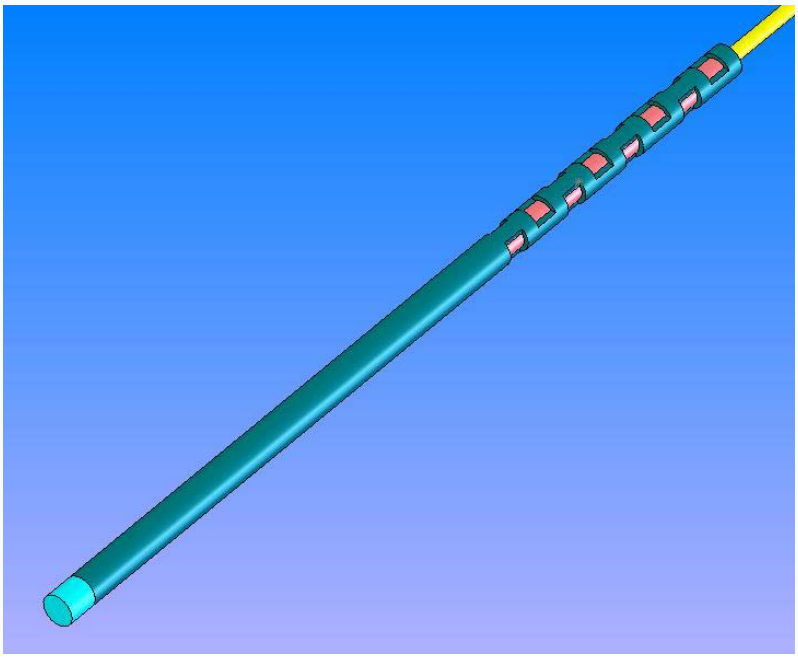

Figure 1. Temperature Sensor, Isometric view

The housing is fabricated from inconel tube stock. The diameter was chosen by determining the size of the components it is to contain and choosing the appropriate standard diameter. The length is determined by the sapphire transducer length, location of the splice between the sapphire fiber and the silica fiber, and additional length necessary to effect an adequate strain relief. The cavity surrounding the sapphire sensing element is kept to a minimum in order to minimize the air space and thus the response time of the sensor. Except for the reflecting element and the first millimeter of sapphire, the entire sapphire assembly is encapsulated in a high-temperature cement, as shown in Figure 2. The encapsulant reinforces the adhesive joints in the transducer fabrication process, eliminates movement within the housing and reduces the effects of shock and vibration on the assembly. The encapsulant material fills the tube to cover the sapphire / silica splice and to retain the Kevlar fibers of the furcation tubing, providing an anchor for the furcation tubing and allowing the fibers to "float" in the central tube (of the Furcation tubing) from the sapphire to the optical connector. The housing tube is slotted towards its distal end in order to reduce conduction through the Inconel from the hot tip end and maximize cooling for the encapsulant (Figure 3). The solid inconel tip is resistance welded to the housing. This is the primary structural element that will be used to attach the sensor to the bracket on the support bars and also to the crossover pipe.

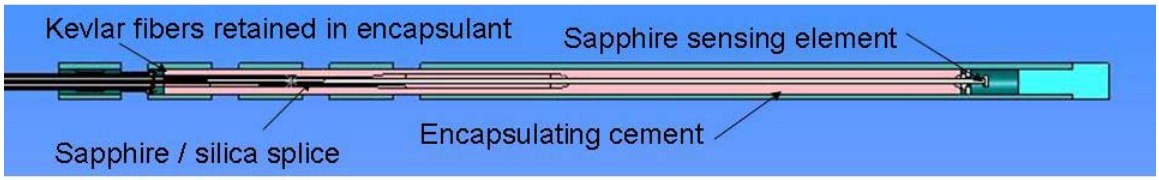

Figure 2. Temperature, Cross section

The sapphire components, inconel tubing, and encapsulant are all capable of withstanding temperatures in excess of 2000° F. Through testing, it was determined that the sapphire / silica splice can withstand temperatures up to ~850° F (450° C). A high temperature laboratory furnace was set to 2000° F (1,093° C). A 4-bore ceramic insulator, equipped with a thermocouple, was installed in an inconel tube with in order to develop a temperature profile, and thus determine a "safe" location for the temperature critical splice. The mock housing was installed through the access hole on top of the furnace. The mock housing was allowed to soak at temperature for an hour before readings were taken. The housing was inserted in ¼" steps into the furnace. Only when the end of the stainless steel housing was within ¼" of the top of the fitting on top of the furnace (and the thermocouple was within 1 ¼") did the thermocouple temperature reading excede 850° F (~450° C). The housing was pulled back ¼" and the reading decreased to 815° F (435° C).

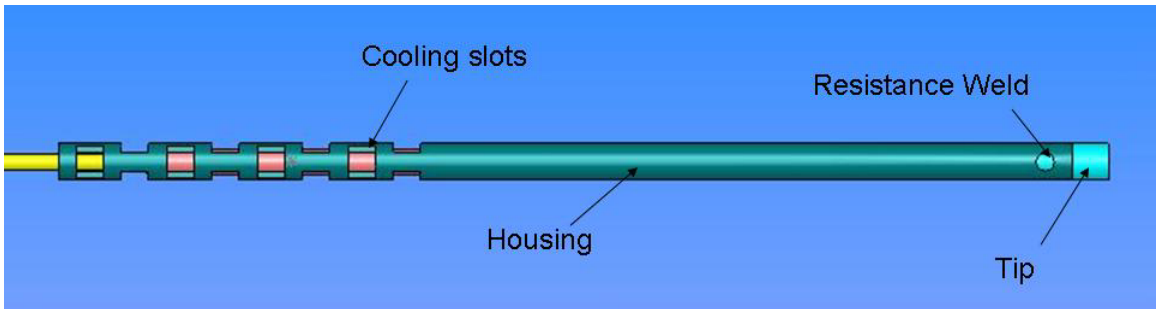

Figure 3. Temperature sensor, side view

Two candidate sites in the Hamilton, Ohio boiler plant for mounting the test sensors were targeted: the first is in the secondary superheater tube bank, and the second is a crossover pipe at the top of the boiler. The first site is on the third floor level. In that location, superheated steam runs through the superheater tubes, high temperature steam runs through the tubes in the membrane wall, the hot gas around the superheater tubes is approximately 2000° F (1093° C), and a nearby soot blower make this severe location an excellent choice to test the sensor in a very aggressive environment. Two temperature sensors will be installed at this location. Steam tubes with ½" thick metal web form the wall. A layer of Kaowool insulation and corrugated sheet metal (Figure 4) cover the wall tubes and form the exterior skin. The floor-level manway (Figure 5) provides convenient access to the test location. Support brackets (Figure 6) provide a location to mount sensors without the need to weld components to operation-critical steam pipes, and possibly compromise their integrity.

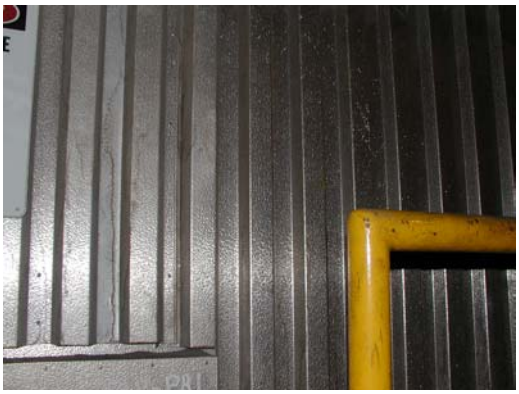

Figure 4. View of Exterior corrugated wall

Figure 5. Manway

An accurate solid model of the steam tubes (Figure 7), supporting brackets and wall was constructed representing the area in which the sensors would be installed for testing. The model was constructed utilizing dimensions from construction blueprints, and photos and dimensions taken at the site.

Figure 6. Secondary superheater tubes and supporting brackets. In this picture, the view is looking up words along the superheater tubes (lower left). The tubes on the right are part of the membrane wall.

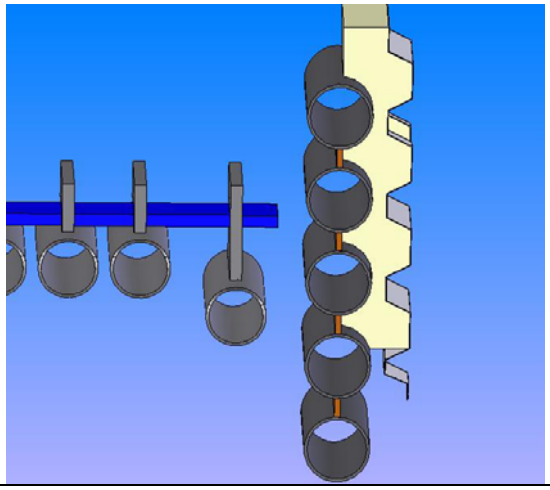

Figure 7. Solid model. In this picture, the membrane wall with its insulation and tubes are on the right, and the superheater tubes are on the left.

It was initially decided to mount one temperature sensor attached to the support bracket. The conduction through the steam pipes to the support brackets would provide the most accurate indication of the pipe temperature, short of mounting it directly on the pipe (which was avoided in order to minimize concerns of the Hamilton, Ohio plant engineers about compromising the reliability of the superheater tubes by welding a sensor directly to the tube).

A 304 stainless steel bracket with multiple temperature sensor mounting holes will be welded to the support bar (Figure 8), and an access slot will be cut into the between pipe web by power plant personnel (Figure 9). The temperature sensor will be installed in this bracket (Figure 10), and an anti-rotation retainer will be resistance welded to this by Prime personnel (Figure 11).

In coordination with Babcock & Wilcox engineers, it was calculated that up to 9" of vertical travel could result from thermal expansion of the steam tubes. A slot will be cut into the web between the pipes to accommodate this movement and a sliding baffle will be installed to minimize the opening to the outside environment.

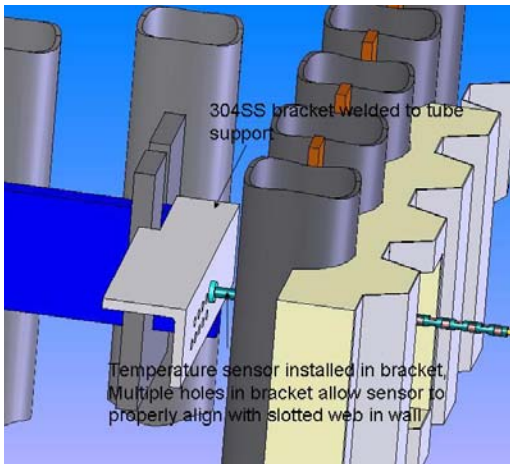

Figure 8. Location of 304 SS bracket, showing temperature sensor installed.

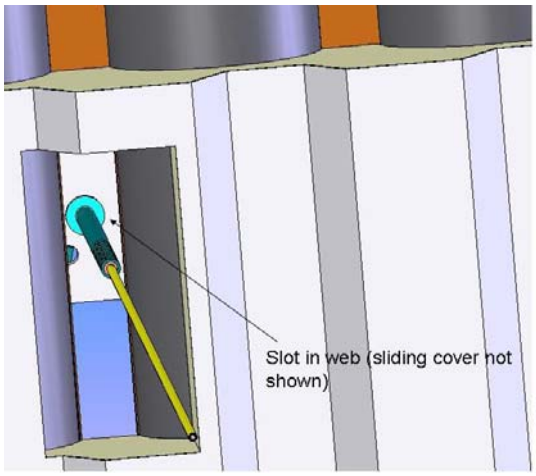

Figure 9. Detail showing slot in membrane wall for exit of the fiber.

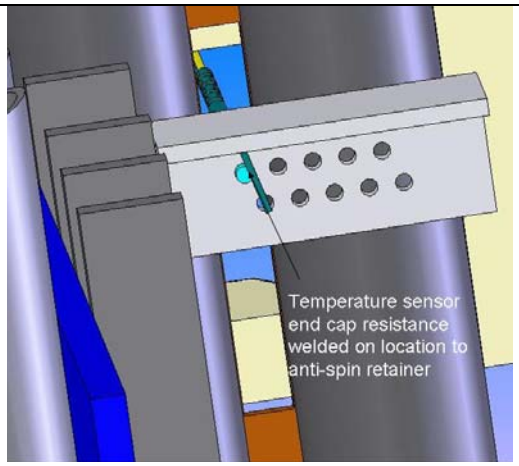

Figure 10. Installation of temperature sensor in 304 SS bracket.

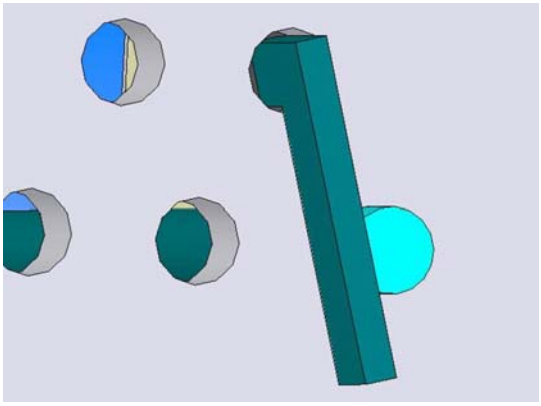

Figure 11. Detail of anti-rotation retainer

We were subsequently informed that horizontal (lateral) travel of the secondary superheater tubes could also be encountered. Babcock & Wilcox engineers provided a video showing the tubes swinging sideways, with an excursion estimated to be in excess of 8 inches. In discussion with the Babcock & Wilcox engineers, it was decided that lateral motion of this magnitude was not likely during normal operation. The motion of the tubes in the video was likely caused by human excitation, since the video showed a work light and extension cord close by the tubes. The presence of the light and cord suggested that the video of the superheater tube motion was not made during plant operation, when temperatures around the light and extension cord would have been about 2000° F. However, the video was useful in that it showed that the superheater tube mounting could not constrained significant lateral motion of the tubes. As a result, we

decided to include backup sensors in a nearby location that would not be subject to damage from horizontal pipe movement.

The additional sapphire temperature sensor will be wall mounted near the support bar mounted unit. A hole will be drilled in the web between wall tubes. The split bushing will be installed from the furnace interior (Figure 12). The spacer will be slid over the split bushing, as shown in Figure 13. The split collar will be installed over the split bushing and pushed tight against the spacer, while the flanged end of the split bushing is pushed up against the furnace interior wall. The split collar will be tightened only enough to retain all components in place (Figure 14). The sapphire temperature sensor will then be slid into the split bushing and the split collar will be tightened to secure the unit (Figure 15).

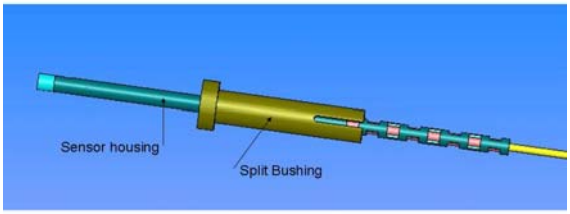

Figure 12. Split Bushing, Thru wall mounting

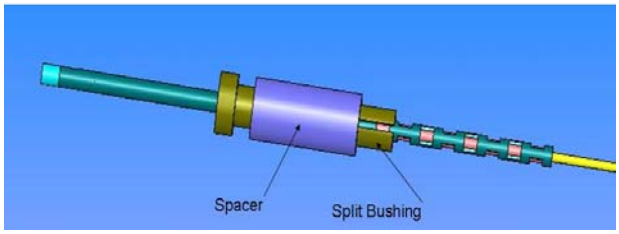

Figure 13. Split Bushing and Spacer

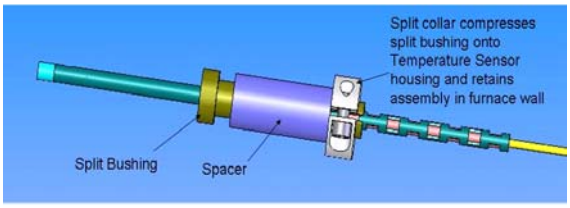

Figure 14. Complete assembly

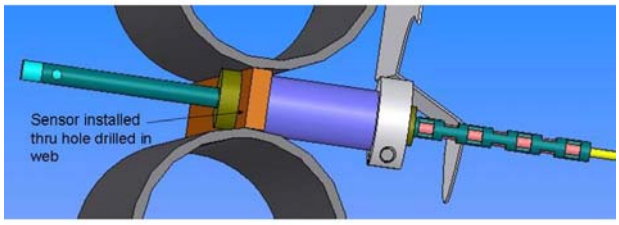

Figure 15. Assembly mounted in furnace

The third location for installation of a sapphire temperature sensor in the Hamilton plant will be on a 15" diameter crossover pipe, which is shown in the photograph in Figure 16. This location was selected due to the ease of access. A saddle will be attached to the pipe and a sapphire temperature sensor will be attached to the saddle (Figure 18 & Figure 19). No drilling or welding will be required for this application. The only preparation required will be to remove a layer of insulation from the pipe at the installation point.

The housing configuration does not change for this application except for the profile of the tip, as illustrated in Figure 17. The contour of the tip is specific for this application only.

Figure 16. Crossover pipe

Figure 17. Detail of tip contour

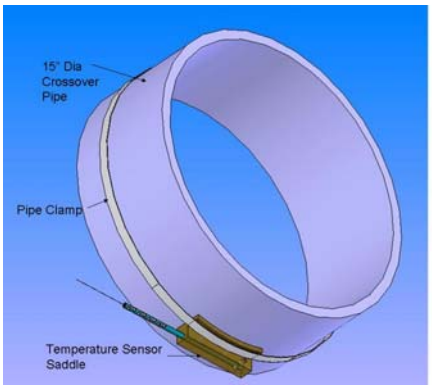

Figure 18. Mounting configuration for crossover pipe

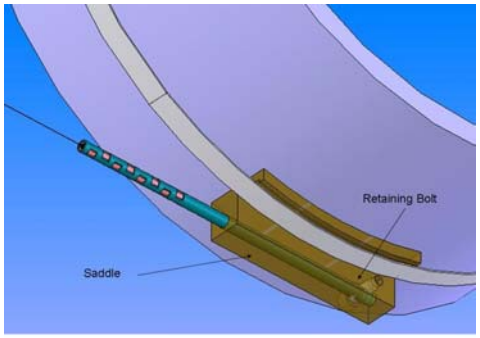

Figure 19. Detail of mounting saddle

3.1.2 Sapphire Strain Gage Development

3.1.2.1 Introduction

During this reporting period, efforts were directed to the development of mechanical assemblies to facilitate the installation of the sapphire Fabry-Perot strain gage developed in the last reporting period and described in the last semiannual report. Goals for the strain gauge package design included easy installation, protection of the sensor, and good transfer of strain from the power plant structure to the strain gage.

The package for the sapphire strain gage was also designed to withstand the high temperatures and corrosive atmosphere of the furnace. The base pad is fabricated of 304 Stainless Steel, the same alloy as the L Bracket shown in Figure 8, and also the same as the pipe support brackets and pipes that make up the power plant. The base pad has recesses on the far face that are sized for nuts which will be used to temporarily attach the strain sensor assembly (Figure 20), and also slots which will accept a custom spot welder electrode, which will effect the permanent attachment of the sensor assembly. The base

pad, with nuts installed, will be flame welded to the L Bracket by certified plant personnel (Figure 21).

The strain sensor substrate (Figure 22) is fabricated from 3/32" thick Inconel plate stock. Two grooves are cut into the plate to accept the sapphire sensor fibers. While only one sensor fiber is needed, the second is redundant in case of failure of the first. Failure may occur during the fabrication or mounting process, or during use. The relative ease of adding a second sensor fiber was instrumental in making this decision. A pair of slots, perpendicular to the fiber grooves, provides the channels necessary for a saw blade to cut the sapphire fibers and make the Fabry-Perot cavity. Again the second slot is redundant, and will only be used if a second attempt is needed to make a clean dicing saw cut through the fiber.

A ¼" outside diameter (OD) inconel tube is attached to the strain sensor substrate (Figure 24). The bottom edge of the tube is tangent to the bottom face of the strain sensor substrate. An inconel block with specific geometry will be the intermediary component providing welding locations for the tube and the strain sensor substrate. A four hole ceramic rod will be installed into the inconel tube. The lower two holes will align with the two grooves in the strain sensor substrate.

A length of clad sapphire fiber is fusion spliced to gold-coated multimode fiber. The multimode fiber is terminated on the other end with an optical connector. This assembly is mounted onto a carrier assembly (Figure 23). A suitable length of the clad sapphire is coated with a suitable metal coating. The coating bonds to the clad surface of the sapphire and provides a conductive surface for the nickel electroplate.

The next step is to prepare the assembly for nickel electroplating. The nickel plating attaches the fibers to the inconel substrate. Nickel bonds to both the inconel substrate and the fibers and is capable of withstanding the high temperature environment of the furnace. The coefficient of thermal expansion of the inconel, a high nickel content alloy, and the nickel plating are almost identical. A sample inconel substrate with coated clad sapphire fibers installed was nickel plated. The adhesion of the nickel plating and fibers to the inconel substrate was successfully tested to 2000 deg F.

The inconel plate assembly with the electroplated fibers is then mounted to film adhesive and hoop for cutting the sapphire fiber in the dicing saw. The plate assembly is attached to the vacuum chuck in the dicing saw, and the chuck is adjusted for tracking the blade centrally through the distal slot in the inconel plate. A cut is made dry (no fluid lubrication) through both fibers. While the Sapphire assembly is still attached and aligned in the vacuum chuck, the connectors are attached to the interrogation system and signal quality is checked. If both sensors show good signal quality the unit is removed from the saw. If both are bad, then a second cut will be made through the fibers in the proximal slot. If one is good a decision will be made based on the quality of the one good signal.

Furcation tubing is installed over the ends of the fibers, and a new connector is installed on each. The end of the furcation tubing in the inconel tube is attached to the inconel tube with high alumina cement. This completes the sapphire strain sensor assembly.

The sapphire strain sensor assembly is then attached to the base pad previously welded to the L Bracket. The procedure will be as follows. From the interior of the furnace, the fibers with connectors are fed out through the slot in the web and the hole in the sliding seal. The sensor assembly is attached to the base pad with two screws. With the custom jaws in the spot welder the sensor assembly is welded to the base pad in four places (Figure 30, Figure 31). Upon completion of welding, the two screws are removed (Figure 32).

An additional Sapphire Strain Sensor (Figure 33) will be wall mounted near the support bar mounted unit. A hole will be drilled in the web between wall tubes. An L bracket will be installed on the wall in the furnace interior. The Sapphire Strain Sensor can be attached to the bracket prior to assembly in the furnace.

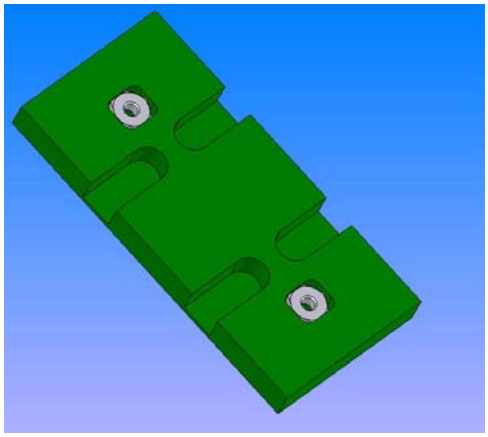

Figure 20. Nuts installed in weld pad

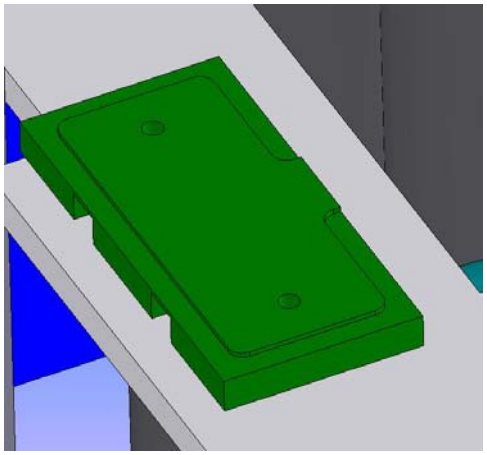

Figure 21. Pad flame welded to L-Bracket in furnace by plant personnel

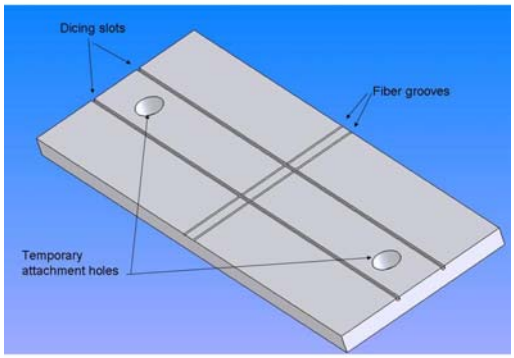

Figure 22. Inconel substrate

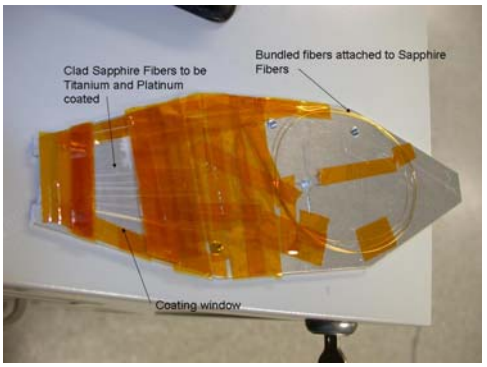

Figure 23. Clad sapphire fibers prepared for platinum-titanium coating

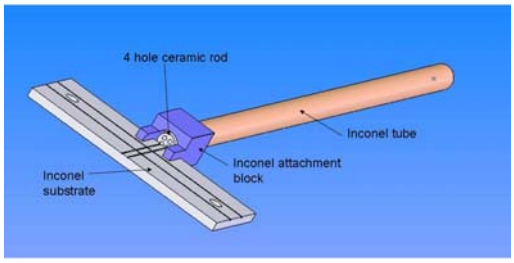

Figure 24. Inconel Substrate with Inconel tube, ceramic rod, and attachment block

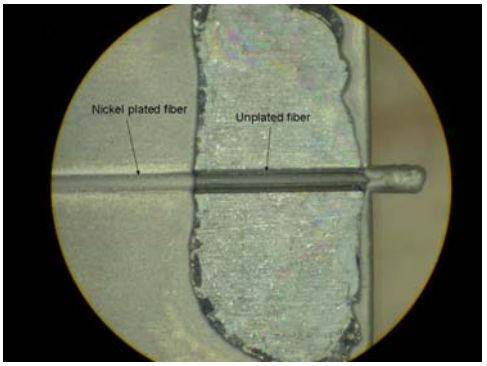

Figure 25. Photo of inconel pad with fiber attached with mask removed after nickel plating

Figure 26. Inconel pad with fibers, after Nickel plating, ready for dicing.

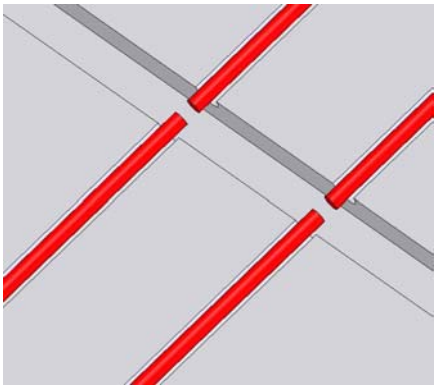

Figure 27. "Diced" fibers form Fabry-Perot sensor

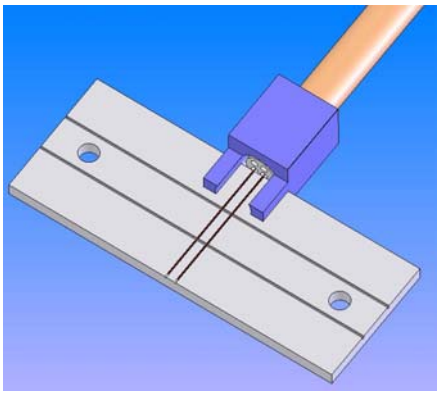

Figure 28. Strain sensor assembly

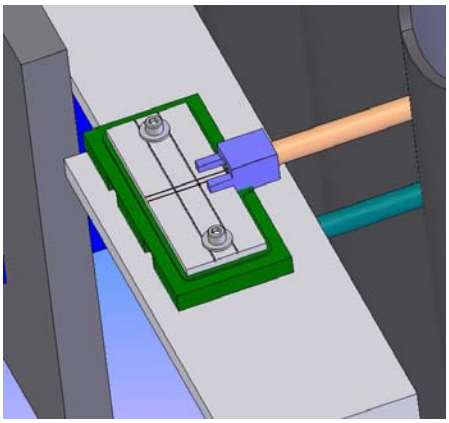

Figure 29. Strain sensor assembly bolted to weld pad

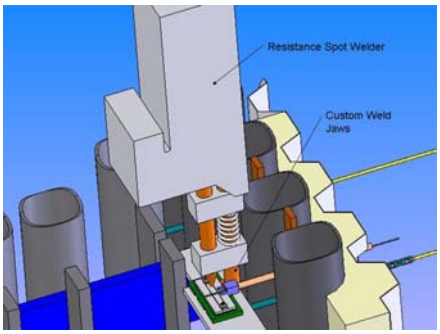

Figure 30. Substrate attached to weld base with spot welder

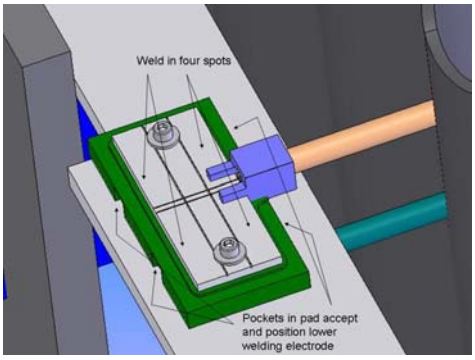

Figure 31. Substrate welded in 4 locations

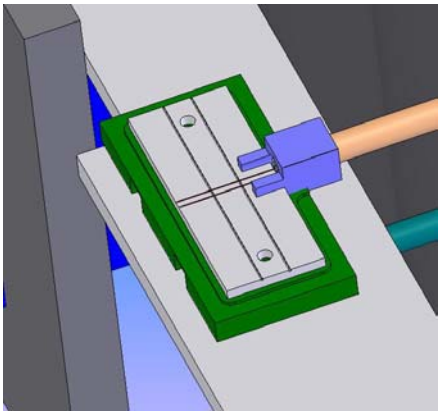

Figure 32. Bolts removed (nuts left in place) after inconel plate resistance welded to weld pad

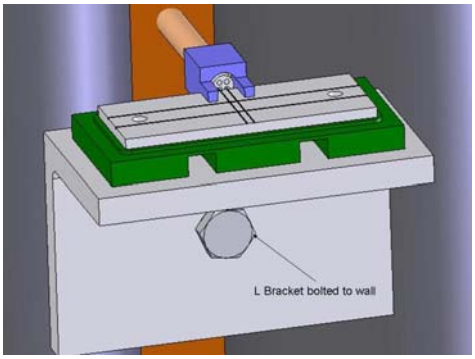

Figure 33. Wall mount Sapphire Strain Sensor

3.1.2.2 Interrogator selection and signal processing

During the reporting period, several methods for interrogating the high-temperature interferometric sensors under development for power plant instrumentation. Two key choices are required in the area of sensor decoding. These two are the question of the interrogation (hardware) methodology, and signal processing (or algorithmic) selection. Three candidates for the interrogation system were evaluated for use in the field demonstration planned for the Hamilton OH plant. Two of these systems are modified versions of existing Prime Research, LC (PRLC) products, the VectorLight™ 200 and VectorLight™ 300. These systems are both based on sensor illumination with a coherent laser source. The required modification to these instruments is to make them compatible with the multimode nature of sapphire fiber.

The third system under consideration is an experimental approach based on broad band illumination with an incoherent light source (a light emitting diode, or LED), referred to as the Experimental Incoherent Interrogator (EII). All three interrogation systems rely on obtaining a spectral response from the transducer. A summary of some basic characteristics of each of these interrogation systems is shown in Table 1 below.

Table 1: Interrogator properties

	VectorLight™200	VectorLight™300	EII
# of simultaneous measurements	1	4	1
Update rate	1Hz	1Hz	4Hz
Wavelength Resolution	2.5 pm	5 pm	~50 pm

In the area of signal processing, there are multiple measures that can be considered in comparison of algorithm suitability. The primary criteria are the algorithm's accuracy, resolution, and whether the algorithm results in an absolute measurement or a relative one. To facilitate clarity, the following definitions are used:

- An absolute measurement is one in which no data regarding the sensor history is required to obtain an accurate measurement of the environment. The sensor may still require a fixed calibration, which would be accomplished upon fabrication.
- A relative measurement is one in which the output of the algorithm indicates the change in measurand between the previous measurement and the current one (e.g. the temperature is now 0.5°C higher than it was one the previous cycle).

To obtain an absolute measurement from a relative measurement requires continuous tracking of the value from a known reference point.

Due to the need to instrument multiple locations in the planned demonstration at the Hamilton boiler plant, a strong preference for systems which result in absolute measurement is logical. This allows for switching between multiple sensors without

having to maintain a dedicated interrogator for each measurement. At this point, emphasis is placed on working with the modified VectorLight™ 200, due to its higher accuracy than the VectorLight™ 300 and because the EII does not currently output an absolute measurement. The data shown and discussed below was all gathered from a modified VectorLight™ 200.

The sensors which are used in this program are in the category of low finesse Fabry-Perot Interferometers. The characteristic spectral response of a low finesse system is a near sinusoidal variation of reflected intensity as a function of wavenumber for a pair of reflective surfaces. Wavenumber k is defined by: $k = 1/\lambda$ where λ is the wavelength of the light being reflected. As additional surfaces are introduced into the sensor, the spectral response grows increasingly complex; the response is the superposition of individual Fabry-Perot cavities formed by all of the surfaces. Theoretical models of the spectra from two and three surface systems can be seen below in Figure 34 and Figure 35, respectively.

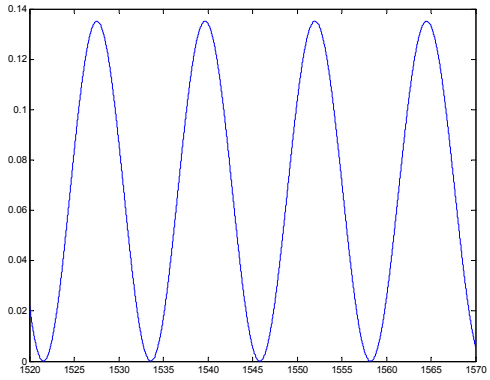

Figure 34: Theoretical simulation of the spectral response from a low finesse *two* surface interferometer

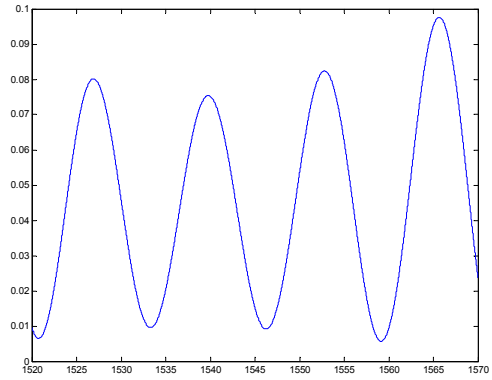

Figure 35: Theoretical simulation of the spectral response from a low finesse *three* surface interferometer

The process of taking a measurement from a given sensor consists of the following steps:

1. Collection of raw spectral data from the reflected signal (Figure 36)
2. Filtering any high frequency noise from the data (Figure 37)
3. Estimating spectral characteristics of the resultant spectrum
4. Correlating those characteristics to measurand.

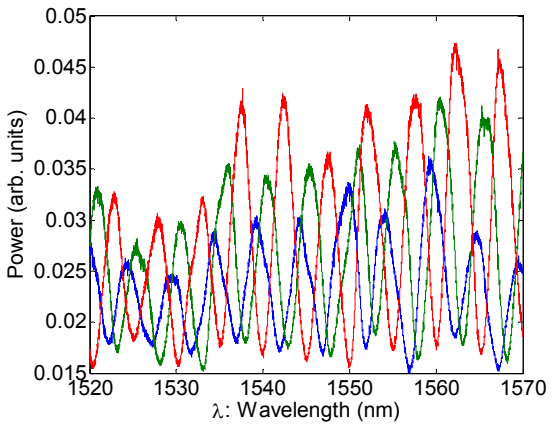

Figure 36: Raw spectral data from temperature sensor at three temperatures

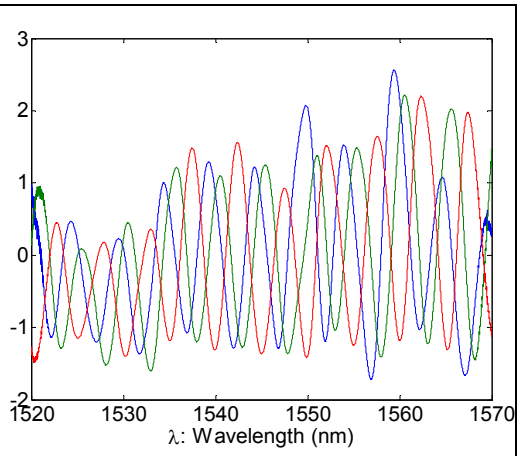

Figure 37: Filtered spectral data of temperature sensor at three temperatures

There are two primary characteristics of these spectra which change as the sensor responds to the measurand (Figure 38). The first is the phase shift which is shown by the marking A. This is a highly sensitive response to changes in the sensor. A problem which it suffers from, however, is that due to the periodic nature of sinusoids, when the measurand traverses a large enough range, it will return to the same value of phase.

The second spectral response is a shift or change in the period (or spacing) between successive peaks in the spectrum (Figure 38 – marked B). This is a much less sensitive measure than the change in phase. As a result, it is substantially more susceptible to noise in the original measurement. It is, however, an absolute measurement, with each value of period correlating to exactly one value of measurand.

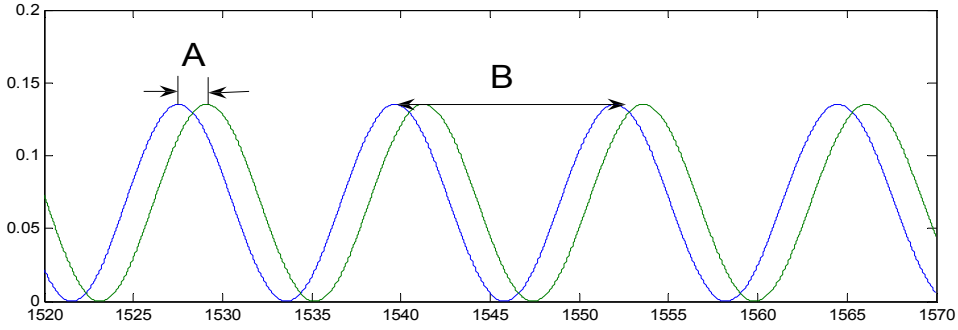

Figure 38: Spectral responses of sensor to measurand: (A) phase shift, and (B) change in period

Processed spectra from a silica pressure sensor and a sapphire temperature sensor can be seen in
Figure 39 and Figure 40 respectively. In both cases, the data shown represent measurements taken at continuously increasing value (although the rate of increase is not constant). The green trace is the calculation of spectral phase. This data is relatively noise free but ambiguous due to the cyclic repeating of values. The blue trace is the optical path length of the sensor, which is a measurement derived from the period of the spectral fringes. This data is noisier, but in the case of the silica sensor, is certainly adequate to distinguish between successive values of phase.

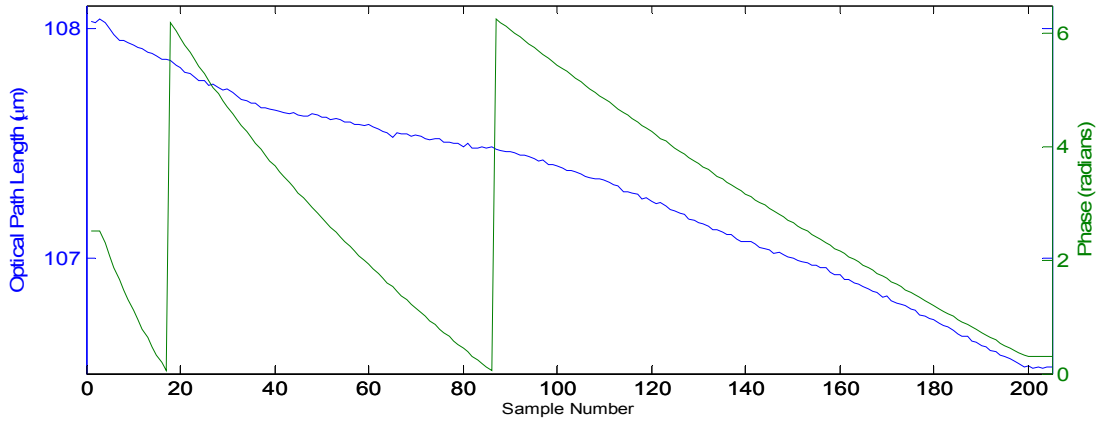

Figure 39: Phase and period measurements from 205 spectra taken from a silica sensor

In Figure 40, one notes that the optical path length measurement is not currently usable for distinguishing between successive values of phase, as it was in the case of the silica sensor. This is the result of errors in calculation induced by the additional noise present in gathering spectra from the sapphire sensor. This is clearly indicated in the comparison of Figure 41 with Figure 42. In Figure 41, it is clear that there are relatively few spectral components, which allows for straightforward separation and detection of signals. The spectra from the sapphire sensor, shown in Figure 42, contain a much richer spectral composition, was well as more variation of that composition from sample to sample. As a result, it is much more difficult to accurately isolate the desired components for analysis.

Work will continue in the area of spectral analysis of the sapphire sensor in the next reporting period. These efforts will include digital filtering to minimize the undesired spectral content in the sapphire sensor's output, and refinements in the optical design to reduce intermodal interference that contributes to the complex spectral content.

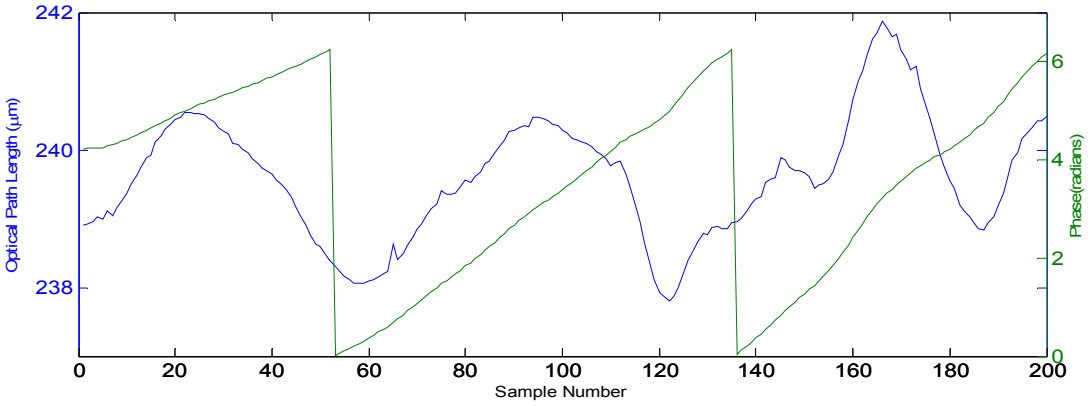

Figure 40: Phase and period measurements from 200 spectra taken from a sapphire temperature sensor

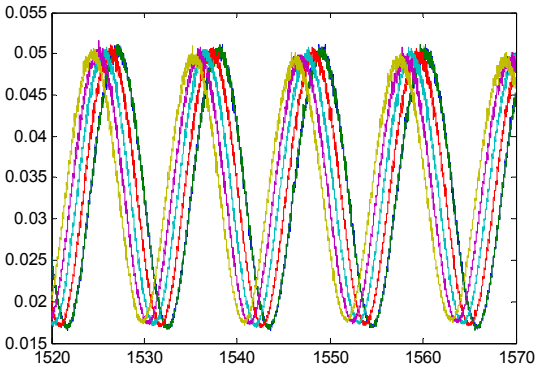

Figure 41: Six sequential spectra taken from silica sensor

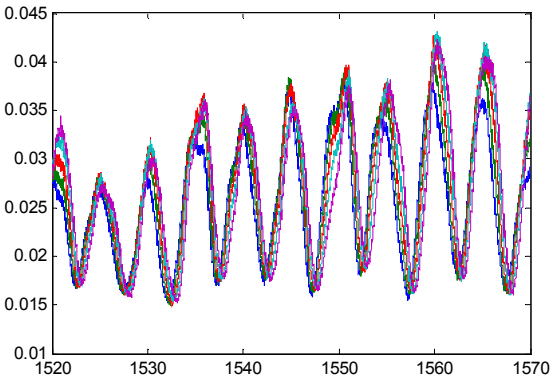

Figure 42: Six sequential spectra taken from sapphire sensor

3.1.3 Silica-to-Sapphire Fiber Splice Development

As described in the last semiannual report, a technique for splicing or joining sapphire fiber to silica fiber was developed. The technique involves using a fused silica capillary tube to align the two fibers, and depositing a hemispherical drop of fused silica glass onto the end of the silica fiber before joining the fibers. The two fibers are inserted into the two ends of the capillary tube using the alignment stages on arc fusion splicer. An arc is used to heat and soften the borosilicate drop, which permits the two fibers to be pushed together. When the assembly cools, the borosilicate glass captures the silica and sapphire fiber is within the capillary to and maintains the optical alignment.

The soft link point of the borosilicate glass establishes the maximum operating temperature of the splice assembly. In order to determine the practical maximum temperature for the splice assembly, and experiment was conducted in which the splice was exposed to a range of temperatures as the sensor output was monitored.

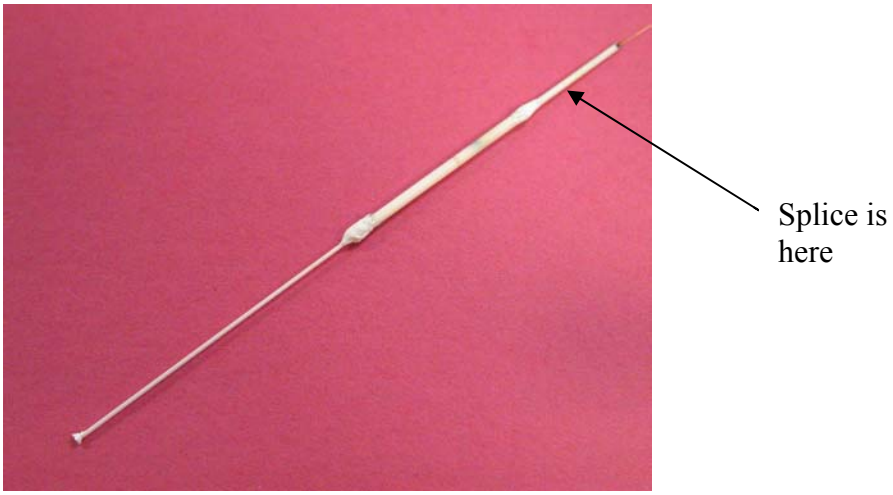

Figure 43. Sapphire temperature sensor in ceramic packaging, showing the location of the silica/sapphire splice.

Figure 43 depicts the temperature sensor in its ceramic packaging. The ceramic is the initial package before the rugged outside housing and final cabling is installed as described in Section 3.1.1. The splice is located in the last section of ceramic tubing (as labeled above).

The first test was assembled according to the photo (Figure 44). The temperature sensor, in its completed ceramic housing, was inserted into the heating coil positioning the splice directly in the center of the heat coil. The coil was controlled by an Omega CNi3244 temperature controller and a variac with an omega thermocouple inserted into the center of the coil. The sensor was connected to a VectorLight 200 interrogator to monitor the sensor output as the temperature was manually increased.

The first temperature was 150° C for 30 minutes to check the fringes. The signal was strong, so the temperature was increased in 50° C steps, allowed to stabilize, and then held for 10 minutes at each temperature. The signal remained strong at each temperature range. Upon achieving 400° C, the temperature was then stepped through more slowly, in steps of 15° C and allowed to stabilize for 15 minutes after each temperature was achieved. At 450° C, a slight drop in the signal was observed, but it still remained a useable signal. The temperature was then increased to 475c. At this temperature, the signal became unstable and within a minute, the signal was completely lost.

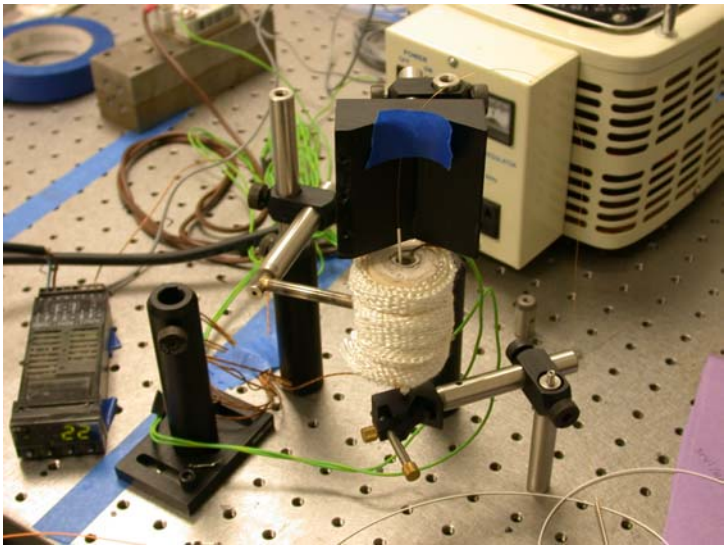

Figure 44. Test set-up to determine maximum operating temperature of the silica-sapphire splice.

The sensor was cooled and successfully unpackaged. After removing the sensor and viewing the splice under a microscope, the adhesive appeared brownish in color. While under the scope, the splice fell apart. The gold fiber cleave was inspected and appeared to be a smooth cleave, therefore confirming the fact that the splice could not handle more than 450° C without failing.

A second test was performed on the temperature sensor splice, but this time without being packaged in the ceramic housing. The bare sensor was inserted in the heating coil with the splice in the center of the coil. The test fixturing and procedure followed was exactly as previous test. The splice failed at 460° C, confirming earlier results.

3.2 Development of Strain Sensors for Solid Oxide Fuel Cell Instrumentation

Prime Research is developing an optical strain sensor required to operate at temperatures up to 800°C (1,472° F) for solid oxide fuel cell (SOFC) applications. Through discussions with NETL researchers, a button cell with a diameter of 1.25 in and thickness of 137 μm has been identified as the substrate. Previous research by NETL predicted that the button cells will have a maximum deflection of 1100 μm. Current sensor technology in use by NETL includes an ITO based thin film strain gauge. This sensor provides a small footprint, low physical and thermal mass, and adequate sensitivity to detect small strain fluctuations. However, the installation process requires specialized equipment to deposit the thin film leads, sensor elements, and lead wire attachments. Prime has identified ease of installation as a requirement for the optical strain sensor under development.

The focus of recent strain gage development efforts over the reporting period has been to utilize the Prime Research Miniature Fabry-Perot Sensor (MFPS) strain gauge and VectorLight™ 200 interrogator for instrumentation of SOFCs. Work thus far has focused on selection and evaluation of adhesives for bonding the strain gage to the substrate, and evaluation of the sensors performance at temperatures up to 800°C. The MFPS strain gage is fabricated utilizing the etch/splice process show in Figure 45; a completed sensor is shown in Figure 46.

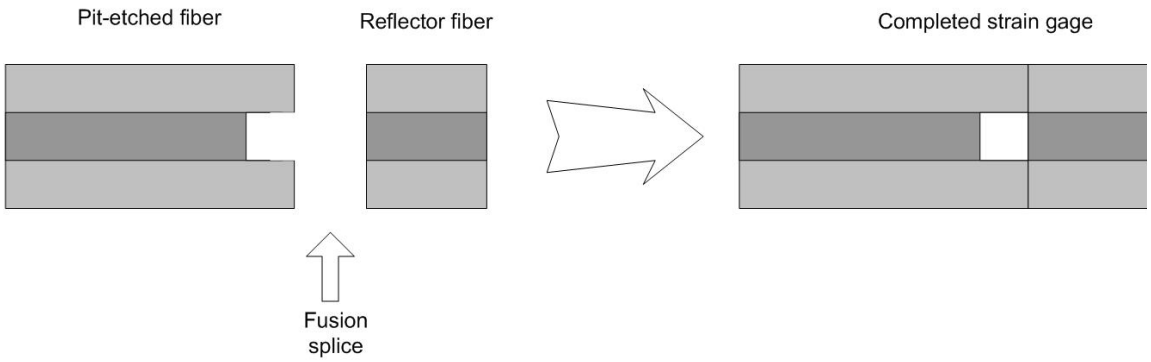

Figure 45. The MFPS strain gage is fabricated by pit-etching a cleaved fiber and then splicing to a reflector fiber.

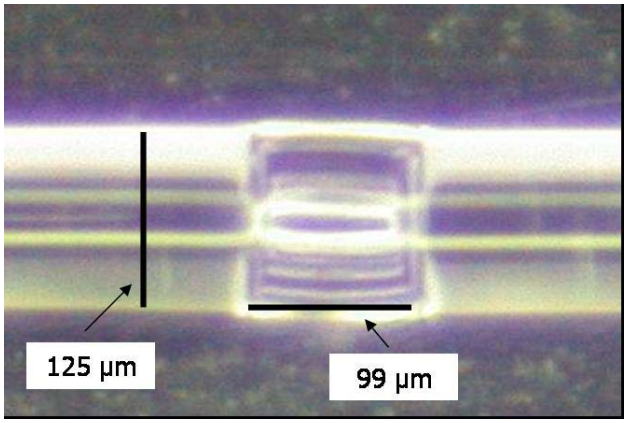

Figure 46. A magnified view of an MFPS strain gage. The 99 µm Fabry-Perot air-gap is noted relative to the fiber diameter of 125 µm.

In order to measure the strain of the fuel cell substrate, the MFPS sensor must be securely bonded to the surface such that any strain induced in the substrate is accurately transferred to the sensor. Initial bonding trials utilized an alumina based adhesive (Aremco 835M) that has a coefficient of thermal expansion (CTE) which approximates that of the fuel cell substrate. The Aremco 835M worked successfully at room temperature but was problematic at elevated temperatures. We suspect that since the CTE of the alumina adhesive is significantly greater than that of the silica fiber, that the mechanical adhesion provided at room temperature was lost at elevated temperatures. Tests showed that at only 100°C, the fiber bonded with Aremco 835M did not accurately transfer strain from the substrate to the fiber. The solution to this problem was found by using a silica based adhesive that has a CTE which approximates that of the silica strain gage. The silica based adhesive utilized was Aremco 618N, and was shown to provide accurate transfer of strain over the full temperature range.

Evaluation of the MFPS strain gage was performed by instrumenting a thin alumina beam and subjecting it to a 3-point bend test. The alumina beams tested were 76 mm long x 13 mm wide x 125 µm thick (3" x 0.5" x 0.005"). For room temperature testing, the alumina beam was suspended between glass rollers and was deflected using a free pivoting blade attached to a digital micrometer. In order to provide a source for comparison, a traditional thin-film electrical strain gage was bonded to the alumina beam at a location of symmetry to the optical strain gage. This room temperature 3-point bend test fixture is shown in Figure 47. A close-up of the alumina beam with electrical and optical gages is shown in Figure 48. Additional insight into the mechanics of the bend test was provided by the Finite Element Analysis (FEA) shown in Figure 49.

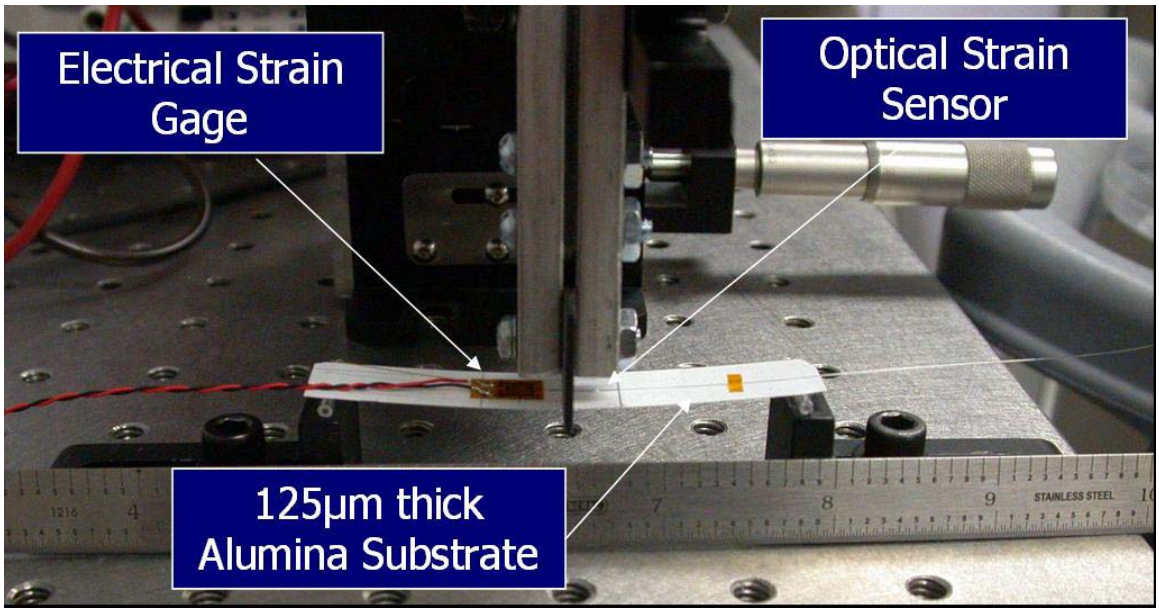

Figure 47. A picture of the 3-point bend test fixture utilized for room temperature evaluation of the MFPS strain gage. The 3" x 0.5" x 125 µm alumina beam is instrumented with an electrical and an optical strain gage which are equidistant from the beam centerline.

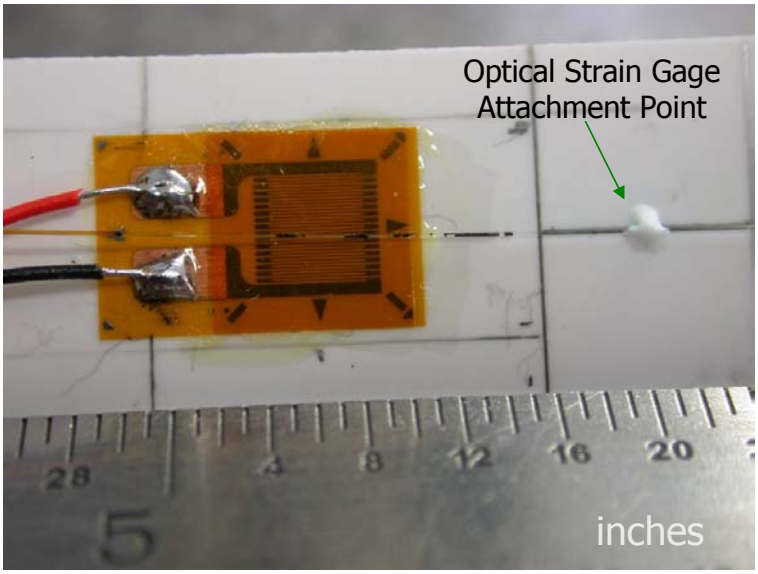

Figure 48. Close-up picture of the 125 µm thick alumina beam instrumented with a traditional thin-film electrical strain gage and a Prime Research MFPS optical strain gage.

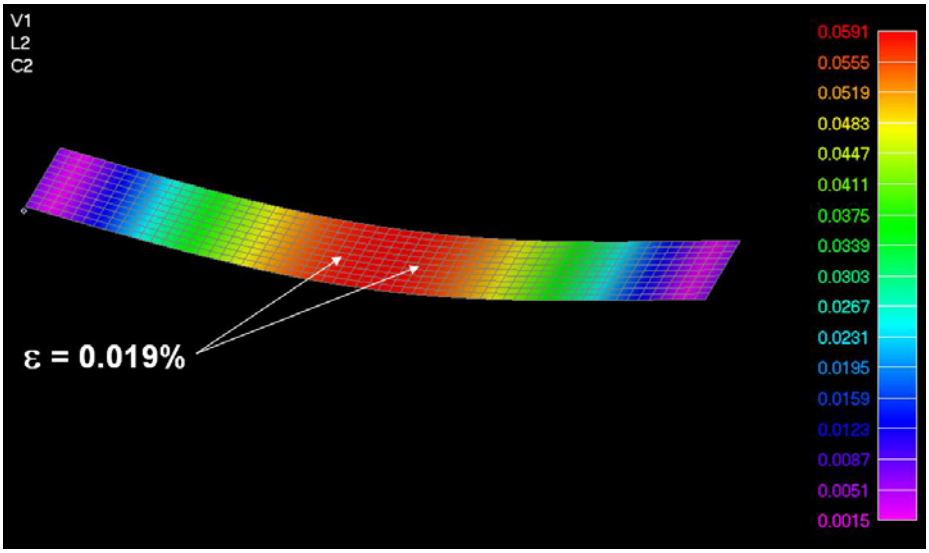

Figure 49. Finite element model of the 3" x 0.5" x 125 µm alumina beam subject to a 1.5 mm centerline displacement. Contours of total displacement (in inches) are shown on a deformed mesh. Displacements are magnified for clarity. The calculated surface strain at the gage installation locations is 0.019%.

The comparison between the electrical and optical measurements, as well as the finite element analysis of the instrumented beam was very good. A plot of measured strain vs. beam centerline displacement is shown in Figure 50.

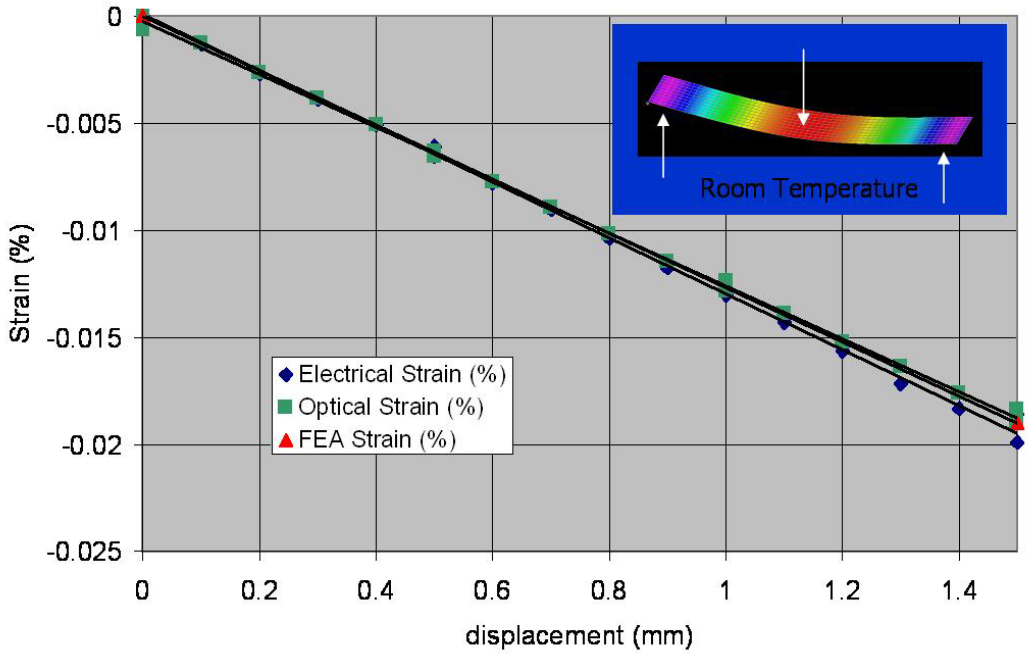

Figure 50. A plot showing the predicted and measured strain vs. beam centerline displacement. The optical and electrical strain measurements are seen to compare well with each other as well as the result predicted by finite element analysis.

After successful demonstration of the MFPS strain gage at room temperature, a test fixture was developed to evaluate performance at temperatures up to 800°C. The fixture was fabricated from alumina tubes and ceramic adhesives; and is meant to provide similar performance to the room temperature apparatus shown in Figure 47. The two prominent differences are that 1) the high temperature fixture's rollers are cemented in place and will therefore impart some frictional forces to the beam; and 2) for the high temperature apparatus, the beam is deflected via an applied load instead of an enforced displacement. The fixture is placed in a standard laboratory box furnace that has access holes in the top and side of the insulated walls. The load is applied to the beam thru the top of the furnace by placing various weights on an alumina pushrod. The strain gage fiber is routed out of the hot-zone thru an access hole in the furnace door. A picture of the high-temperature 3-point bend test fixture is shown in Figure 51.

In order to study the high temperature performance, two MFPS optical strain gages were bonded to the alumina beam with Aremco 618N. After performing the cure cycle required by the adhesive, the beam was heated to 800°C and a strain test was performed two times. Each strain test consisted of the following steps: 1) add the pushrod (12.28 grams), 2) add 10 grams weight, 3) add 10 grams weight, 4) remove 10 grams, 5) remove 10 grams, 6) remove the pushrod (12.28 grams). A plot of the sensor response as a function of time to these two strain tests is shown in Figure 52.

Figure 51. A picture showing the high temperature 3-point bend test fixture inside the box furnace. The 3" x 0.5" x 125 µm alumina beam is supported on alumina tubes; the load is applied from the top via the guided alumina pushrod. A penny is shown at the right for scale.

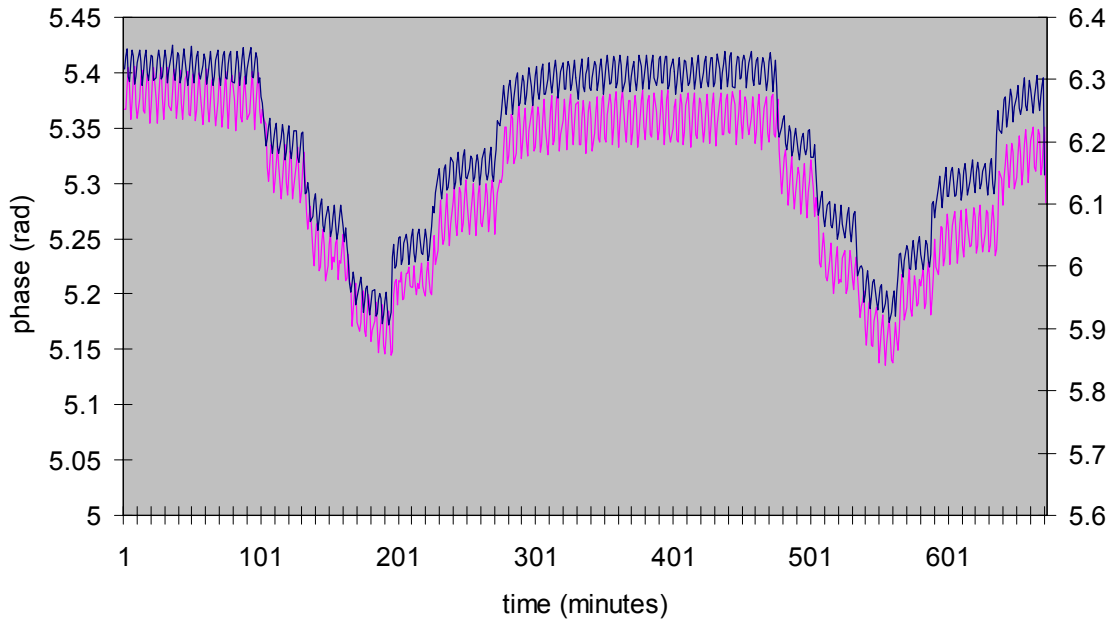

Figure 52. A plot showing the response of two MFPS optical strain gages to a strain test. The sensor response in radians is plotted as a function of time. The strain test was performed by applying 3 incremented weights and then removing them. The test was performed twice.

3.2.1 Development of Distributed Sensors for Solid Oxide Fuel Cell Instrumentation

In addition to the strain gage work intended for SOFC button cell applications, Prime Research is developing sensor technologies for use in full-size fuel cells.

During this reporting period, Prime Research worked toward completing Task 11 and began work on Task 12.1 in the contract statement of work. Task 11 involves determining the requirements for sensor approaches that will help researchers experimentally validate their analytical models of solid oxide fuel cell systems. Task 12.1 involves selecting the most promising application for development, then designing optical probes for that application, including optical sensors for distributed measurements.

3.2.1.1 The need for distributed sensors

Current fuel cell technology utilizes stacks of ceramic plates that must withstand both the rigors of heating and the pressure of gaseous reactants, in addition to the forces used to compressively seal the fuel cell stack. Heating ceramics from room temperature to fuel cell working temperature causes thermally induced expansion that can easily crack the ceramic plates that must be also be clamped together to keep reactant gasses from escaping. When one plate in a stack fails, the entire stack becomes non-functional. Therefore, researchers have a strong need to understand both the mechanism of failure and the underlying reasons for it, with the ultimate goal of making more robust designs.

Once a fuel cell is at working temperature, fuel gas and compressed air are introduced to begin the generation of electricity. As these gasses flow, they are generally at a lower temperature than the fuel cell and cause a shift in the temperature profile across the cell, further complicating the issues of thermally induced stack failure. This change in temperature profile also affects the rate and efficiency of the cell reactions, which results in the generation of more or less additional reaction heat across the cell profile. The combination of these factors makes theoretical modeling a complex task. Without a way to measure the actual fuel cell cross-sectional strain and temperature profile, no real world validation of theoretical results is possible.

Much of the research and development in fuel cells up to now has been with stacks of modest dimensions, for example, a square approximately 17 cm on each side. However, as energy conversion plants scale up for bulk production, fuel cells with a larger cross sectional area are clearly needed. Knowledge about how temperature and strain profiles affect the failure rate of ceramic materials will become increasingly important in the future.

What is needed, then, is a large number of sensors in a tight distribution across the cross-sectional area of a fuel cell, because it is the minute variations in cell temperature and strain that is important, not just a single bulk measurement. Any form of electrical type sensor technology would require a large number of wires to carry the profile information from the hot zone out to where the data can be used. With high temperatures, ceramic plates, and glass seals involved, this wiring represents a significant logistical challenge.

For example, if the fuel cell stack working area is 17 cm by 17 cm, and a spatial resolution of 1 cm is needed, then this represents a need for 289 sensors, which for electrical sensors would likely call for 578 wires.

In the case of fiber optic sensors, a large number of sensors can be built into a single fiber and read out using an instrument located far away from the hot zone. A sensor plate can be prepared in advance, and then installed in the stack during assembly, with only one or two optical fibers going to the outside. The result would be an easy-to-implement multi-sensor solution that will enable researchers to understand stack parameters better, even as stack cross sectional area increases.

3.2.1.2 Distributed sensor technology

With the clear need for many sensors on a single fiber, Prime Research has examined how this has been done in the past and how a fresh approach might advance the state of the art in this area. First, a survey of existing technologies was undertaken, including both single sensor approaches and multiple sensor approaches. Table 2 below indicates the results of that survey so far.

Table 2. Survey of Sensor Applicability

	Ease of Manufacturing	Applicability for Pressure Measurement	Applicability for Temperature Measurement	Applicability for Strain Measurement	Cost of Development	Multiplexibility	Resolution	Limitations
FBG	high	poor	good	very good	moderate	very good	very good	Requires IP licenses
LPG	high	moderate	good	moderate	moderate	moderate	moderate	Requires IP licenses
IFPI + OTDR	high	poor	good	good	moderate	good	poor	Slow response, poor resolution, poor stability, only tested to 300 C ,
IFPI + SLI	high	poor	very good	very good	moderate	moderate	very good	Maximum of 10 sensors, only tested to 300 C
EFPI	moderate	good	good	very good	low	moderate	very good	Maximum of 10 sensors
Microbend	high	good	moderate	moderate	low	poor	poor	
OFDR	low	poor	good	good	high	very good	good	limited to short distances
DTS	moderate	not applicable	very good	not applicable	high	very good	very good	limited to <250 ºC
Polarimetric	low	moderate	good	good	low	poor	moderate	Requires special fibers
Black Body Radiation	moderate	not applicable	very good	not applicable	moderate	poor	moderate	

IFPI = intrinsic Fabry-Perot interferometer
FBG = fiber Bragg grating
OFDR = optical frequency domain reflectometer
DTS = distributed temperature sensor
EFPI = extrinsic Fabry-Perot interferometer
SLI = swept laser interrogation

When multiple sensors are placed on one fiber, the mechanism for determining one sensor response from another is called the discrimination method.

Fiber Bragg Gratings, as shown in the table, are easy to manufacture, widely available and well understood, but they suffer from several limitations. When wavelength division multiplexing is used as the multi-sensor discrimination method, the conveniently available spectral width (provided by telecommunication components) limits the number of sensors that can be put in one fiber to the order of tens of sensors. In addition, most gratings are fabricated in photosensitive germanosilicate fiber. Such Type-I gratings are manufactured using either continuous wave or pulsed UV laser irradiation, resulting in color centers that change the index of refraction of the core. Because of this method, Type-I gratings suffer from signal fading effects and are essentially erased at approximately 200^{O}C. This is a moderately high temperature for a telecommunications environment, but a relatively low temperature compared to the solid oxide fuel cell environment.

Optical Time Domain Reflectometry (OTDR) methods work well when the structures are large because the discrimination method is the time of flight for an individual pulse of light. Any change of index of refraction encountered along the fiber causes a light reflection that returns to the instrument. The exact time of the return of the reflection depends upon how far down the fiber the index of refraction change is from the instrument. Light travels very fast, so even fast electrical timing methods translate into long physical distances, much larger than the dimensional scale of solid oxide fuel cells.

Extrinsic Fabry-Perot Interferometric have been the subject of extensive development, but the extrinsic nature of their construction makes multiplexing difficult due to the high optical losses of each sensor element.

Intrinsic Fabry-Perot interferometry does not suffer so much from the light loss issue, because the light is confined to the optical fiber. However, IFPI cavities written using methods similar to Type-I Fiber Bragg Gratings also suffer from signal fading above 200 ºC. Due to the similarity in fabrication methods for FBG sensors and IFPI sensors, it is likely that persistent IFPI sensors suitable for use at the higher temperatures can be fabricated through the use of a high-power excimer laser.

3.2.1.3 Direction of research

At this point in our investigation, the use of intrinsic Fabry-Perot cavities appears to be the best direction moving forward to build a realizable system. Although previous investigations of IFPI sensors have demonstrated some limitations, we plan to work in two areas to extend the technology:

1. Extend the working temperature range of IFPI sensors by changing the mechanism of reflection to one that does not suffer from the fading problems associated with Type-I Fiber Bragg Gratings.

2. Remove the multiplexibility limitation of only a few sensors, as when wavelength division is used as a discrimination method. By changing the discrimination method to a swept wavelength to spatial transform, the entire light spectrum can be used for all sensors. A Fourier transform can then be used to resolve one IFPI cavity apart from the other cavities by their different cavity lengths.

3.2.1.4 Extending the Temperature Range

When Fiber Bragg gratings are written into photosensitive fibers using a UV laser, minute structural changes in the fiber are created. These structural changes cause a strong reflection when made in the form of a Bragg grating. However, these effects are significantly reduced if the fiber is exposed to temperatures above 200 ºC.

Instead, when gratings are formed using a very intense, single pulse of light (>500mJ/cm^2), such as with a high-power excimer laser, Type-II gratings are obtained. Type-II photosensitivity is caused by the resulting damage at the core-cladding interface. This fusion of the glass matrix at the writing point is a highly nonlinear dynamic process. Type-II photosensitivity can lead to a refractive change as high as 1%. Gratings made a using a Type-II process show great stability at high temperature, withstanding temperatures as high as 800^{o}C without erasure.

There is a threshold of pulse energy density of about 650mJ/cm^2 where the Type-II effect begins. When the pulse energy is below this threshold, refractive index changes linearly with energy density. Above this threshold, the refractive index change increases dramatically with increasing energy density. When the pulse energy is higher than 1000mJ/cm^2, the refractive index change effect begins to saturate.

Because of this damage at the interface of fiber core and cladding, the fiber becomes somewhat fragile at the writing point. This fragility may limit the applicability of a Type-II sensor as a tensile strain gage.

By changing the mechanism of the reflection from color centers as in Type-I gratings to structural decomposition as in Type-II gratings, we expect to be able to extend the working reflection temperature to 800 ºC, where solid oxide fuel cells operate.

3.2.1.5 Mechanism of Interrogation

Removing the multiplexibility limitation of wavelength division discrimination is clearly the most challenging part of this research effort. Wavelength division discrimination only allows a few sensors to be placed on a single fiber because the spectrum is carved up into narrow regions, one for each sensor. This forces a trade-off between sensor range and the number sensors. By using a spectral to spatial transform, all sensors can use the entire spectrum. The location of the sensor along the fiber acts to distinguish that sensor from all the others.

The details of this discrimination mechanism and the new limiting factors are still under investigation at this time. Construction of a prototype interrogator can begin when more detail is available about how wide a spectral range is needed and how narrow the

interrogating laser line width needs to be. These parameters will also likely drive the update rate / frequency response of the interrogation system. When experimental data becomes available, the details of this spatial transform analysis will indicate just how many sensors can be placed in the fiber and discriminated individually using a particular interrogation system.

4 Plans for Future Work

During the next reporting period, prototype sapphire sensors will be assembled for installation in the Hamilton, Ohio boiler plant. With assistance from Babcock & Wilcox engineers, the sensors will be installed during the shutdown of the plant during the winter 06/07 season. A total of three sapphire strain gauges and three sapphire temperature sensors will be installed in the plant. Work will continue on the improvement of spectral processing for the VectorLight 300 interrogator, and software were be developed to enable remote monitoring of the VectorLight 300 output during the field test. Data from the sensors will be logged during the plant operation in late spring and early summer 2007 for further analysis.

Demonstration of the MFPS strain gage for mechanical valuation of SOFC button fuel cells at 800° C will be performed. The use of an excimer laser for the fabrication of persistent, high-temperature IFPI sensors for distributed measurement of temperature and/or strain in SOFC fuel cell elements will continue, and development of signal processing techniques for the demultiplexing of IFPI sensors concatenated on a single fiber will begin.